2010 IEEE International Conference on Robotics and Automation
Anchorage Convention District
May 3-8, 2010, Anchorage, Alaska, USA

Experimental Investigation of Effects of Flapping Wing Aspect Ratio and Flexibility on Aerodynamic Performance

Chengkun Zhang, Zaeem A. Khan, Sunil K. Agrawal*
MechSys Lab, Department of Mechanical Engineering
University of Delaware, Newark (19716), DE, USA

***Abstract*—In earlier studies, the optimal wing kinematics that gives the best aerodynamic performance was determined with a robotic flapper. The geometry and physical properties of wings are also critical for designing and fabricating Flapping Wing Micro Air Vehicles (FWMAVs). In this paper, the effects of wing aspect ratio and flexibility on aerodynamic performance are experimentally investigated to determine the optimal aspect ratio for Micro Air Vehicles (MAVs) wings at Reynolds number around 18,000. The comparison between the aerodynamic performance of rigid wings and flexible wings are also made whose veins are fabricated out of different materials.**

I. Introduction

Due to its promise for carrying out missions such as search and rescue in collapsed structures, surveillance and reconnaissance, the field of Micro Air Vehicles (MAVs) is attracting an increased number of researchers [1][2]. Conventional MAVs with fixed wings or rotary wings can be designed by scaling down full sized aircrafts to provide attractive solutions for the aforementioned missions. However, biomimetic flapping wing micro air vehicles (FWMAVs) offer a number of advantages over conventional MAVs such as high maneuverability and the capability for sustained hover flight. These are ideal for accomplishing MAV missions, especially in tight space.

Over the past two decades, a lot of researchers have aimed at developing biomimetic FWMAVs that generate insect-like wing motion. Some examples are Berkeley micro mechanical flying insects [3][4], Harvard robotic insect based on Diptera [5].

Apart from the development of FWMAVs, experimental biologists have also studied optimal geometry and kinematics of wings of insects and birds. Ellington's works on revolving wings show that even radical changes in model hawk moth wing forms have relatively slight effect on aerodynamic properties [6]. Dickinson explored wing rotation and aerodynamics of insect flight by a dynamically scaled model of fruit fly, Drosophila melanogaster [7]. Chai have studied hummingbird flight performance by examining its flight in a suite of experimental studies [8][9][10]. Our group at University of Delaware has designed and fabricated a robotic flapper to systematically study the aerodynamics of flapping wings. Optimal kinematic parameters for a wing of fixed geometry were studied using the robotic flapper [11].

* Corresponding Author: Dr. Sunil K. Agrawal from ME in University of Delaware, Newark, DE, USA (19716) agrawal@udel.edu

Undoubtedly, research on wing geometric properties and kinematics will greatly advance the development of FWMAVs. Among those researches, Heathcote and Gursul studied the effect of span-wise flexibility on the thrust, power-input and propulsive efficiency of a rectangular wing which is rigid along the chord-wise direction [12]. One observation from previous literature is that insects, such as hawk moth, use *small aspect ratio* wings operating at Reynolds Number (Re) less than 7000, whereas hummingbirds use *large aspect ratio* wings at $\mathrm{Re} \approx 18,000$. We want to study the question why hummingbirds, with much larger Re number, fly with wings having larger aspect ratio compared to insects. The effects of wing aspect ratio and flexibility on the aerodynamic performance will be explored in this paper.

The rest of this paper is organized as follows: The wing kinematic model and aerodynamic performance criterion are presented in section II. The optimal wing kinematic parameters, which are used in the series of experiments in this paper, are also briefly summarized in this section. In section III, the experiment setup is introduced in detail. Section IV presents two sets of experiment results. Comparisons between wings of different aspect ratio and rigidity are made in section V with results and important conclusions. Discussion is made as well in this section to compare this study with the relevant works done by other researchers.

II. Wing Kinematics and Aerodynamic Performance Criteria

A. Wing Kinematic Model

This section presents an insect wing kinematic model based on Euler angles. First, the important geometric parameters are introduced. As shown in Fig. 1, leading edge is the upper most section of the wing.

Half of the wing span (R) is defined as the length from the base to the tip of the wing. The area of the wing can be calculated as

$$S = 2\int_0^R c\,dr. \tag{1}$$

The aspect ratio (AR) of the wing is obtained by the formula:

$$AR = \frac{4R^2}{S} = \frac{span^2}{wing\ area} \tag{2}$$

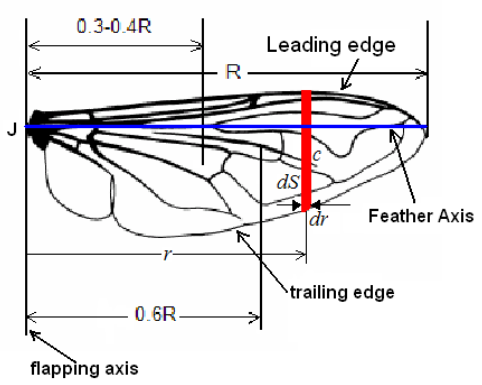

Fig. 1. Typical insect wing

For the typical wing motion of small insects, there are three fundamental modes of motion excited by the thorax, called the flapping angle θ_f, deviational angle β and rotational angle θ_r respectively. The wing kinematics is built on the assumption that the wing is a rigid flat plate with motion described by the flapping angle θ_f and rotational angle θ_r respectively. The magnitude of deviational angle β, also known as the stroke plane tilt angle, is considered small compared to θ_f and θ_r and its aerodynamics effects have been found to be negligible [13]. In order to develop the wing kinematic model, a coordinate system $\mathbb{F}_{\mathrm{W}}:(\hat{x}_w,\hat{y}_w,\hat{z}_w)$ is attached to the rigid wing as shown in Fig. 5 with the origin denoted by B located at the wing base.

The earth fixed frame $\mathbb{F}_{\mathrm{o}}:(\hat{x}_o,\hat{y}_o,\hat{z}_o)$ is shown in Fig.3, where the unit vectors $(\hat{x}_o,\hat{y}_o)$ describe a horizontal plane parallel to the earth, $\hat{y}_o$ is normal to the plane of symmetry of insect body and $\hat{z}_o$ is along the gravity direction. Fig. 3 also gives the sensor coordinate system $\mathbb{F}_4:(\hat{x}_4,\hat{y}_4,\hat{z}_4)$. The wing frame $\mathbb{F}_{\mathrm{W}}$ can be described by three successive rotations with respect to the inertial frame $\mathbb{F}_{\mathrm{o}}$ as shown in Fig. 2 A, B and C. Fig. 2 describes how to rotate the global frame to the wing frame by a sequence of rotations.

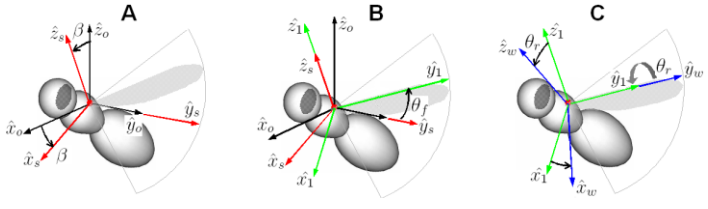

Fig. 2. Sequence of rotation $(\beta,\theta_f,\theta_r)$ which describes the stroke plane inclination, and wing motion.

An important parameter related to the flapping motion is the stroke amplitude Θ_f, defined as

$$\Theta_f=\frac{1}{2}(\theta_f^{\max}-\theta_f^{\min}). \tag{3}$$

Finally, the Reynolds number can be determined from Eq. (4) based on geometric property and operating parameters of the wing:

$$\mathrm{Re}=\frac{8\Theta_f R^2 f}{\nu AR}. \tag{4}$$

where f is the flapping frequency, ν is the kinematic viscosity of the fluid. Re number lie between 5,000 and 10,000 for large insects and within the range from 12,000 to 20,000 for hummingbirds. Re number approaches 10 for the smallest insects. The robotic flapper used in this study is designed for Reynolds number 11,000-18,000. For dynamic similarity and also based on the data from the literature [9], the robotic flapper experiments presented in this paper were conducted at $\mathrm{Re}=18,000$ so that the FWMAV with a similar size as hummingbird is operated at similar Reynolds number.

B. *Aerodynamic Performance Criterion*

The criterion for good aerodynamic performance is high lift at a high lift by drag ratio. High lift is required for weight support and carrying useful payload while high lift by drag ratio determines how efficiently the wings generate lift at the cost of expenditure of energy. The lift and drag forces vary during the wing beat cycle. Therefore, cycle averaged lift and drag are used. The cycle averaged coefficients of lift and drag are given respectively by

$$C_L=\frac{\bar{L}}{1/2\rho S_2\pi^2(f\Theta_f)^2}, \tag{5}$$

$$C_D=\frac{\bar{D}}{1/2\rho S_2\pi^2(f\Theta_f)^2}. \tag{6}$$

where S_2 is the second moment of wing area given by Eq. (7).

$$S_2=2\int_0^R r^2c(r)dr. \tag{7}$$

in which $c(r)$ is the chord length for the element at a r distance from the base of the wing as shown in Fig. [1].

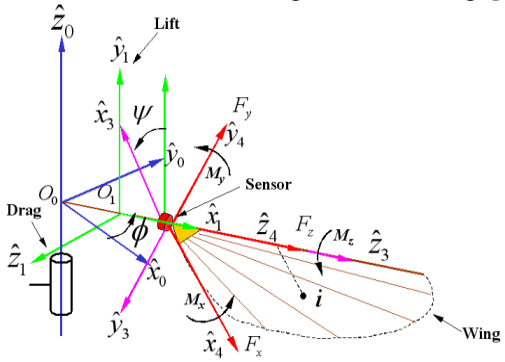

Fig. 3. Sensor coordinate system $\mathbb{F}_4$, lift force and drag force coordinate system $\mathbb{F}_1$ of the robotic flapper

The numerators of Eq. (5) and Eq. (6) are the cycle averaged lift force $\bar{L}$ and drag force $\bar{D}$, which can be obtained by the following equations:

$$\bar{L} = \frac{1}{T}\int_0^T L(t)dt, \quad \bar{D} = \frac{1}{T}\int_0^T |D(t)|\,dt. \tag{8}$$

Lift force $L(t)$ and Drag force $D(t)$ are force components along the $\hat{y}_1$ and $\hat{z}_1$ direction respectively as shown in Fig.3. Note that absolute value of drag is used since drag cancels out during one wing beat cycle. Then, the lift to drag ratio can be denoted as $\bar{L}/\bar{D}$ since the denominators in Eq. (5) and Eq. (6) are the same.

Therefore, the criterion for aerodynamic performance is high coefficient of lift C_L at a high lift by drag ratio $\bar{L}/\bar{D}$.

C. Determined Optimal Kinematic Parameters

The typical wing time trajectory of Θ_f and θ_r in this experiment is shown in Fig. 4, where the flapping angle Θ_f is chosen as a sinusoidal function of time.

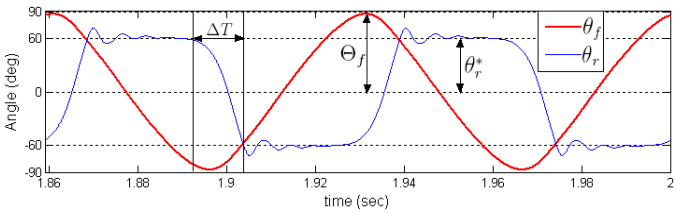

Fig. 4. The typical wing time trajectory of Θ_f and θ_r

The wing kinematics can be described by a few parameters which allow the variation in kinematics without changing it qualitatively. As shown in Fig. 4, these parameters are the stroke amplitude Θ_f, the angle of attack $\alpha^* = \pi/2 - \theta_r^*$, the phase shift ϕ_r between the flapping motion and rotational motion. The speed of rotation or duration of rotation ΔT is a fraction of wing beat cycle time period during which flip occurs.

Previous work by Khan and Agrawal was to determine the optimal wing kinematic parameters to maximize aerodynamic performance [11]. This current study used some key results in [11] such as the flapping angle, the rotation angle and the phase difference between the flapping and rotation angles. Some of these results are:

1. *A compromise has to be made between achieving maximum lift capability (high C_L) and high $\bar{L}/\bar{D}$ ratio because maximum averaged lift coefficient C_L and lift to drag ratio $\bar{L}/\bar{D}$ do not occur at the same parameter values.*

2. *Maximum θ_f increases both C_L and $\bar{L}/\bar{D}$.*

3. *Advanced flip ($\phi_r > 0^\circ$) increases both $\bar{L}/\bar{D}$ and C_L. However, while C_L increases almost linearly with ϕ_r, maximum $\bar{L}/\bar{D}$ occurs at $\phi_r \approx 10^\circ$.*

4. *Finally, maximum $\bar{L}/\bar{D}$ occurs $\beta = 0^\circ$ (horizontal stroke plane).*

In the series of conducted experiments, the flapping magnitude was chosen as $\theta_f = 90^\circ$, which is its maximum physical limit to avoid the wings colliding with each other. Angle of rotation was selected as $\phi_r = 15^\circ$. The change of deviation angle will affect the aerodynamics of the flapping wing slightly. In this study, we chose the deviation angle to be zero, which means that the stroke plane is horizontal.

III. Experiment Setup

To characterize the aerodynamics of flapping wings, a robotic flapper system was designed and fabricated.

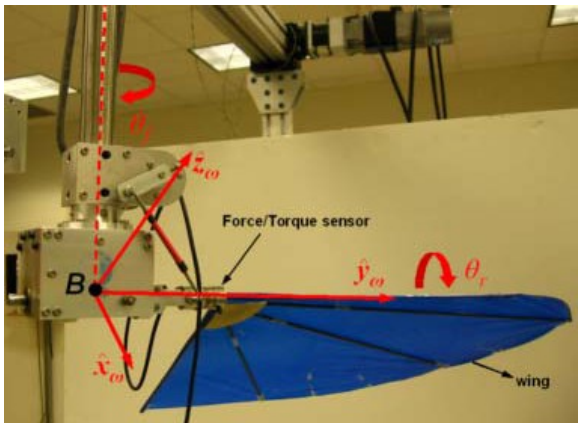

Fig. 5. The robotic flapper driven by three independent servo motors and can generate $(\theta_f, \theta_r, \beta)$ wing motions.

In the experiments, this robotic flapper was used to investigate how the aspect ratio and rigidity affect the aerodynamic performance of the wing. As shown in Fig. 5, it consists of three independent motors controlling the three degrees of freedom $(\theta_f, \theta_r, \beta)$ respectively to generate insect like wing motion. The degree of freedom controlled by β was locked in the experiments because the deviation angle was chosen as 0°, as mentioned in Section II. The controller of this flapper drives the other two motors according to the reference kinematics. It has a 6- axis force and torque sensor mounted at the base of the wing which is responsible for capturing the forces and torques generated by the moving wing.

To fulfill the aim of the series of experiments, four wings were fabricated at the same time with exactly the same

geometric configuration, as shown in Fig. 6. Two of them are rigid wings, whose veins were fabricated with very stiff but light weight hollow carbon tubes. One of the rigid wings was covered with membrane made of thin mylar and the other one without.

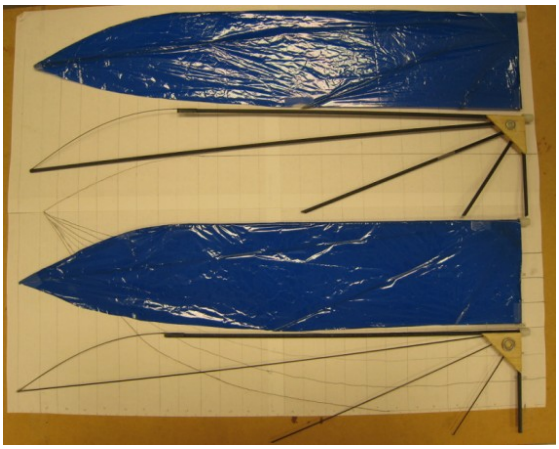

Fig. 6. Two rigid wings and two flexible wings.

The other two wings are flexible wings, whose leading edge and root edge are made of highly stiff carbon rods whereas the veins are made of thinner and flexible carbon fiber rods. One of the flexible wings is covered with membrane and the other one is without the membrane. The wings without membrane were used to cancel the gravitational forces and inertial forces and torques acting on the corresponding wings with membrane so that we can tease out the net aerodynamics forces and torques.

Initially, we fabricated four wings with leading edge length R as 35cm and root edge length as 25cm. For each wing, we did the experiment by altering the angle of attack from 10° to 70° at a 5° interval. Then we cut them smaller by shortening the length of root edge. The root edge length of all of the wings was cut shorter from 25cm to 10cm at a 2.5cm interval. Totally, we have seven sets of wings with different aspect ratio, as shown in Table 1. Each set of wings consists of two rigid wings and two flexible wings, all with the same size and shape.

Table 1. Geometric parameters of seven wings in the Experiment

Wing set	Wing Span/2	Root Edge	Aspect Ratio
1	50.1cm	25cm	4.83
2	50.1cm	22.5cm	5.36
3	50.1cm	20cm	6.02
4	50.1cm	17.5cm	6.90
5	50.1cm	15cm	8.04
6	50.1cm	12.5cm	9.54
7	50.1cm	10cm	11.55

IV. Experiment Results

We conducted two sets of experiments. In Experiment 1, we aimed to investigate the effects of wing aspect ratio on the aerodynamic performance of the wing and attempted to find the optimal aspect ratio for wings of MAVs at Reynolds number around 18,000. Hence, rigid wings of seven different aspect ratios are compared with respect to the key parameters of aerodynamic performance including coefficient of lift C_L and lift to drag ratio $\bar{L}/\bar{D}$. On the other hand, we explore the effects of wing rigidity on the aerodynamic performance in Experiment 2 by comparing the key parameters of aerodynamic performance of rigid wing with its corresponding flexible wing which has exactly the same size and shape as the rigid one.

To minimize the experimental errors, the robotic flapper is run until the real-time curves stabilize. Then forces and moments are collected for 15 periods of flapping motion. Later, ten periods of wing motion are picked from this sample and then averaged.

The sensor data is filtered on-line using a first-order filter and off-line with a zero-phase delay low-pass Butterworth filter. After teasing out the net aerodynamic forces and torques acting on the wing with membrane, we transform them from the sensor coordinate system $\mathbb{F}_4$ into the coordinate system $\mathbb{F}_1$ as shown in Fig. 3. Then Eq.5, Eq. 6 and Eq. 8 are used to calculate the key aerodynamic performance parameters such as C_L, C_D and $\bar{L}/\bar{D}$.

Due to the large volume of data, only a portion of the experiment results are shown in this section:

Experiment 1

The coefficients of lift C_L for wings with different aspect ratio at different angle of attack are shown in Fig. 7.

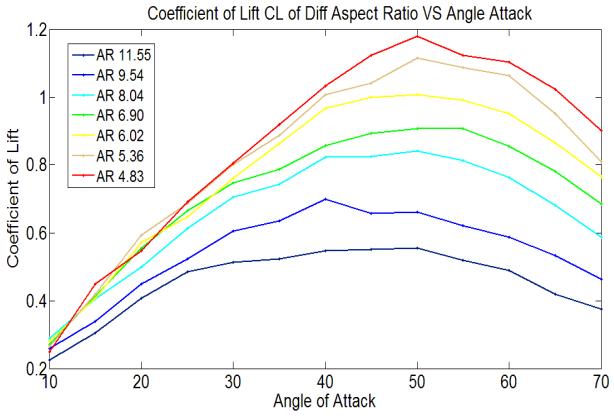

Fig. 7. Coefficient of lift of seven rigid wings at different angle of attack.

The coefficients of drag C_D for wings with different aspect ratio at different angle of attack are shown in Fig. 8.

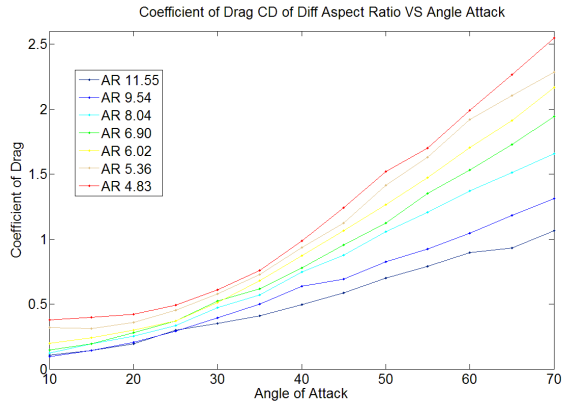

Fig. 8. Coefficient of drag of seven rigid wings at different angle of attack.

The lift to drag ratio $\bar{L}/\bar{D}$ for wings with different aspect ratio at different angle of attack are shown in Fig. 9.

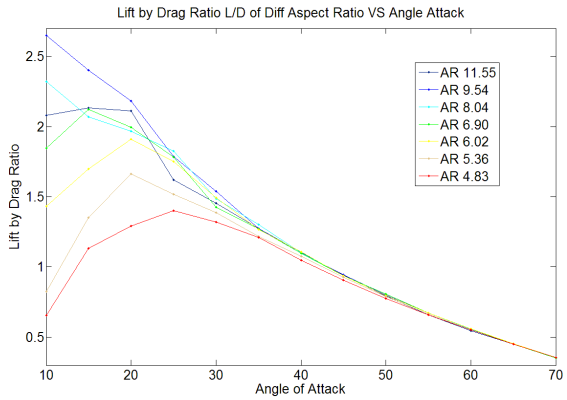

Fig. 9. Coefficient of lift by drag ratio of seven rigid wings at different angle of attack.

Experiment 2

C_L for rigid wing and flexible wing with aspect ratio AR=6.90 at different angle of attack are shown in Fig. 10.

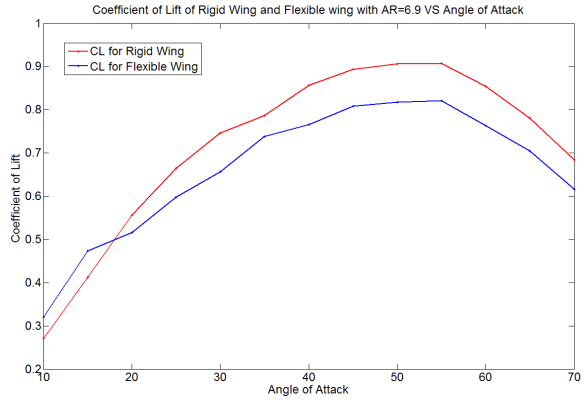

Fig. 10. Coefficients of lift for rigid wing and flexible wing with AR=6.9 at different angle of attack.

Lift by drag ratio $\bar{L}/\bar{D}$ for rigid wing and flexible wing with aspect ratio AR=6.90 at different angle of attack are shown in Fig. 11.

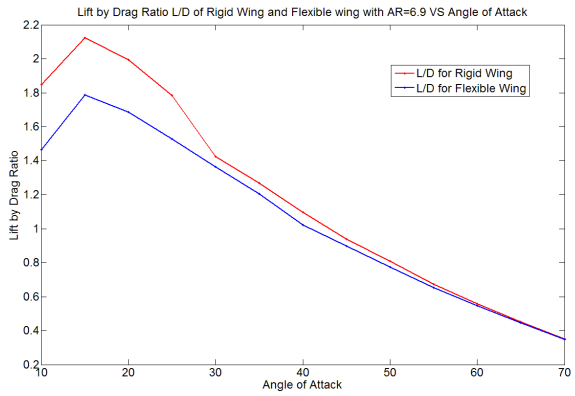

Fig. 11. Lift by drag ratio for rigid wing and flexible wing with AR=6.9 at different angle of attack.

C_L for rigid wing and flexible wing with aspect ratio AR=5.36 at different angle of attack are shown in Fig. 12.

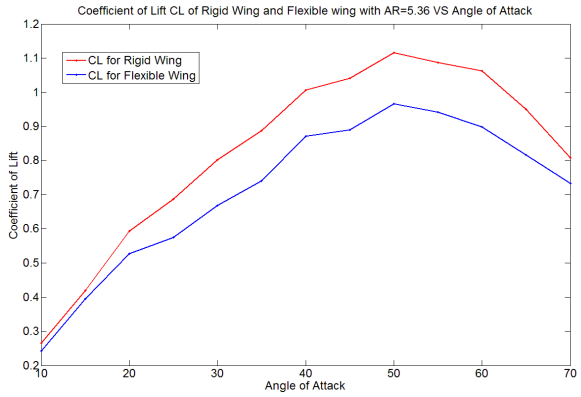

Fig. 12. Coefficients of lift for rigid wing flexible wing with AR=5.36 at different angle of attack.

Lift by drag ratio $\bar{L}/\bar{D}$ for rigid wing and flexible wing with aspect ratio AR=5.36 at different angle of attack are shown in Fig. 13.

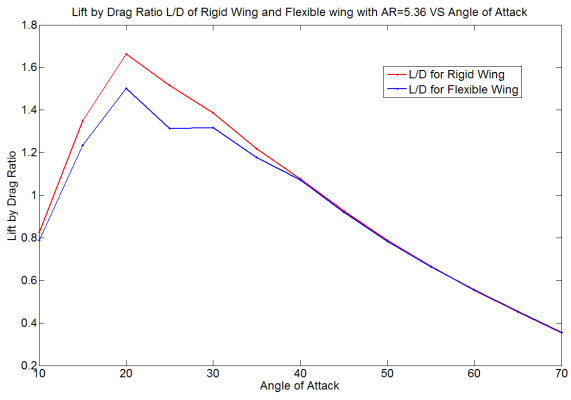

Fig. 13. Lift by drag ratio for rigid wing and flexible wing with AR=5.36 at different angle of attack.

V. Discussions and Conclusions

We find some unexpected, but interesting results when exploring the effect of wing aspect ratio on its aerodynamic performance. The maximum coefficient of lift C_L for wings with different aspect ratio occurs at different angles of attack. Moreover, there is no striking difference in the lift by drag ratio $\bar{L}/\bar{D}$ between seven wings at angles of attack larger than 40°. However, substantial differences in the lift by drag ratio are seen in seven wings at smaller angles of attack. The wings with AR=9.54 or AR=8.04 give the best aerodynamic performance at small angle of attack based on one of the key aerodynamic performance criterion—lift by drag ratio.

One of the most interesting findings in this paper is that the largest lift to drag ratio happens to the wing which has an aspect ratio close to hummingbird wings. Based on the plan form images of real hummingbird wings of *Selasphorus rufus*, the aspect ratio roughly is AR=8.88 [14]. Note that our experiments have Reynolds Number (Re=18,000) close to those of hummingbirds.

Ellington found no significant effect of aspect ratio in insect wings based on his revolving wing experiments with wing models of hawk moth [6]. However, our experiments indicate that *large aspect ratio* is better for improving aerodynamic performance as seen in Hummingbird's wings.

Healthcote et al demonstrate that an intermediate flexibility can benefit the wing performance by increasing the thrust coefficient and propulsive efficiency [12]. Furthermore, they hypothesize that birds, bats and insects may benefit aerodynamically from the flexibility of their wings.

When examining the effects of rigidity on the wing aerodynamic performance with biologically mimicking wings, we find that forces and torques are smoother for flexible wings than rigid wings. These plots are not shown in the paper but were intuitively expected. However, the aerodynamic performance of the rigid wings is slightly superior to that of the corresponding flexible ones. This was clearly out of line from our expectations.

From the previous study of MAVs, we anticipated that the flexible wings would have better aerodynamic performance than rigid ones. As a matter of fact, the flexible wings with smaller aspect ratio have a slightly smaller lift by drag ratio $\bar{L}/\bar{D}$ for angle of attack larger than 40° whereas have a striking smaller lift to drag ratio $\bar{L}/\bar{D}$ for small angles of attack. The data collected in the experiment demonstrate that the flexible wings do not offer aerodynamic advantages over rigid wings. This is unexpected but is consistent with the most updated research on the effect of wing flexibility on the aerodynamic force generation of flexible wings by Zhao [15]. In hindsight, we altered the aspect ratio of the wing by cutting the root edge and the trailing edge in the series of experiments. This changed the shape of the wings. Our future studies will attempt to keep the shape of the wing unchanged and only change the size.

In addition, it is also of interest to study the influence of operating frequency on flapping wing aerodynamics performance in the future work.

VI. ACKNOWLEDGMENTS

The authors gratefully acknowledge funding from National Science Foundation (NSF) in support of this work.

REFERENCE

[1] Zbikowski, R., Galinski, C., Pedersen, C. B., "Four-Bar Linkage Mechanism for insect-like Flapping Wings in Hover: Concept and an Outline of its Realizations", Journal of mechanical design, July 2005, Vol 127.

[2] Banala, S. K, Agrawal, S. K., "Design and Optimization of a Mechanism or Out-of-plane Insect Wing-like Motion With Twist. Journal of mechanical design", July 2005, Vol 127.

[3] Taylor, G. K. "Mechanics and aerodynamics of insect flight control" Biol. Rev. Camb. Phil. Soc. 76, 449-471, 2001.

[4] Deng, X., Schenato, L., Wu, W. C., Sastry, S. "Flapping Flight for Biomimetic Robotic Insects: Part I System Modeling", IEEE Trans. On Robotics, vol. 22, no. 4, August 2006

[5] Wood, R. J. "The First Takeoff of a Biologically Inspired At-ScaleRobotic Insect", IEEE TRANSACTIONS ON ROBOTICS, VOL. 24, NO. 2, APRIL 2008

[6] Usherwood, J.R., Ellington C.P., "The aerodynamics of revolving wings I. model hawkmoth wings", Journal of Experimental Biology, 2002 Jun; 205(Pt 11): 1547-64.

[7] Dickinson, M. H., Lehmann, F. O., and Sane , S. P., "Wing rotation and the aerodynamic basis of insect flight" , Science, vol. 284, pp. 1954-60, Jun 18, 1999.

[8] Chai, P., Harrykissoon, R. and Dudley, R. (1996). "Hummingbird hovering performance in hyperoxic heliox: effects of body mass and sex", J. Exp. Biol. 199, 2745-2755.

[9] Chai, P., Chen, J. S. C. and Dudley, R. (1997). "Transient hovering performance of hummingbirds under conditions of maximal loading", J. Exp. Biol. 200, 921-929.

[10] Chai, P., Dudley, R., "Maximum Flight Performance of Hummingbirds: Capacities, Constraints, and Trade-Offs", VOL. 153, No. 4, THE AMERICAN NATURALIST, April, 1999.

[11] Khan, Z., Agrawal, S. K., "Modeling, Optimal Kinematics, And Flight Control Of Bio-Inspired Flapping Wing Micro Air Vehicles", Doctoral Thesis, University of Delaware, 2009

[12] Healthcote, Gursul, "Effect of span-wise flexibility on flapping wing propulsion", Journal of Fluids and Structure, 2008.

[13] Sane, S. P. and Dickinson, M. H., (2001). "The control of flight force by a Flapping Wing: Lift and Drag Production", Journal of Experimental Biology, 204, 2607-2626 (2001)

[14] Douglas, L., Dudley, R., Ellington, C. P., "Aerodynamic forces of revolving hummingbird wings and wing models", J. Zool., Lond. (2004) 264, 327-332.

[15] Zhao, L., "The effect of chord-wise flexibility on the aerodynamic force generation of flapping wings: experimental studies", IEEE International Conference on Robotics and Automation, 2009.